Small-angle scattering studies of the fully hydrated phospholipid DPPC

P. C. Mason and B. D. Gaulin

Department of Physics and Astronomy, McMaster University, Hamilton, Ontario, Canada L8S 4M1

R. M. Epand

Department of Biochemistry, McMaster University, Hamilton, Ontario, Canada L8N 3Z5

G. D. Wignall and J. S. Lin

Center for Small-Angle Scattering Research, Oak Ridge National Laboratory, Oak Ridge, Tennessee 37831

Small-angle neutron and x-ray scattering studies have been carried out on fully hydrated dipalmitoylphosphatidylcholine (DPPC) multilamellar vesicles. This system is known to exhibit two distinct ripple ($P_{\beta'}$) phases, which depend on sample history, at temperatures intermediate to its high-temperature liquid crystalline (L_α), phase, and its low-temperature gel ($L_{\beta'}$), phase. On cooling from the L_α phase, the $P_{\beta'}$ phase displays a complex multipeak diffraction pattern that differs significantly from the diffraction pattern seen in the $P_{\beta'}$ phase obtained on warming from the $L_{\beta'}$ phase. Examining the $P_{\beta'}$ phase on cooling using small-angle neutron scattering and x-ray diffraction techniques leads to the conclusion that this phase is characterized by a long wavelength ripple ($\lambda_r \sim 330$ Å) and a highly monoclinic unit cell ($\gamma \sim 125°$). As the $P_{\beta'}$ phase is traversed in temperature, the ripple wavelength changes significantly while the monoclinicity remains unchanged. Ripples from the $P_{\beta'}$ phase are seen to persist into the $L_{\beta'}$ phase on cooling, leading to increased small-angle scattering characteristic of a disordered stacking of the lamellae. [S1063-651X(99)11101-2]

I. INTRODUCTION

The rich phase behavior of phospholipid bilayers and their structural relationship to biological membranes have motivated scientists from many disciplines to examine their unique properties. In excess water, phospholipids self-assemble into multilamellar vesicles (MLVs) consisting of concentric, stacked bilayers each separated by a layer of water. The repetition of structure lends itself well to diffraction studies. Perhaps the most scrutinized of all model membranes, dipalmitoylphosphatidylcholine (DPPC) continues to be a source of intrigue. In particular, the novel ripple ($P_{\beta'}$), phase of DPPC (and other PCs) has been the source of much recent study and debate [1–4]. The $P_{\beta'}$ phase, characterized by the development of a long periodicity corrugation of the bilayer lamellae, is an intermediate phase spanning a relatively narrow (~8 °C) temperature range between the low-temperature gel ($L_{\beta'}$) and high-temperature liquid crystalline (L_α) phases. Among the fascinating properties of this phase is its nonequilibrium behavior reported by Tenchov, Yao, and Hatta [5] in which the diffraction pattern obtained after slowly cooling the sample from the L_α phase is markedly different than that seen after warming the sample into the $P_{\beta'}$ phase from the $L_{\beta'}$ phase.

Yao *et al.* [6] concluded that the $P_{\beta'}$ phase on cooling in DPPC consists of two coexisting ripple structures. Their model proposes that there is phase coexistence between regions of the ripple phase identical to that obtained on warming, and regions for which the ripple wavelength is approximately two times greater. The diffraction pattern would then be a superposition of the patterns obtained from each of these regions. In this paper we discuss small-angle neutron and x-ray scattering studies of fully hydrated DPPC in the temperature regime (~20 °C–50 °C) wherein it displays all three of the $L_{\beta'}$, $P_{\beta'}$, and L_α phases, paying particular attention to the $P_{\beta'}$ ripple phase and the history dependence of the structure within this phase. While our diffraction data are similar to those obtained by Yao *et al.* [6], we show that both our data and those obtained by Yao *et al.* [6] can be understood in terms of a well-ordered, highly monoclinic, single wavelength structure occurring on cooling, and a less-well-ordered single wavelength structure occurring on warming. In addition, we show that a related history dependence exists for the $L_{\beta'}$ phase, with disordered ripples persisting into the $L_{\beta'}$ phase when it is entered from above in temperature.

II. MATERIALS AND EXPERIMENTAL METHODS

1,2-dipalmitoyl-sn-*glycero*-3-phosphocholine (DPPC) and DPPC in which the quaternary ammonium methyl hydrogens have been replaced with deuterium (DPPC-d_9) were purchased from Avanti Polar Lipids, Inc. (Birmingham, AL) and used without any further purification.

For the small-angle neutron scattering (SANS) experiments, 50 mg of DPPC-d_9 was suspended in 0.5 mL D$_2$O/PIPES buffer [20 mM piperazine-*N*,*N'*-bis[2-ethanesulfonic acid], 1 mM ethylenediamine tetraacetic acid (EDTA), 150 mM NaCl in D$_2$O adjusted to a *p*H meter reading of 7.4]. This buffer simulates physiological conditions. The solution was centrifuged and transferred to a 1 mm path length Helma quartz cell and incubated at 45 °C for at least 24 h. Excess water was drawn off and more suspension was transferred into the cell. After incubating a second time, a small amount of water was visibly separated from the remainder of the solution, confirming that the sample was in a state of excess water. An undeuterated
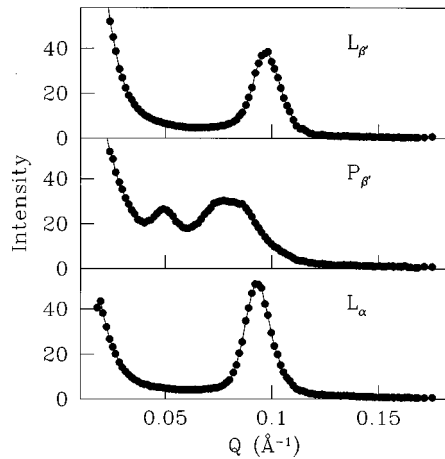
FIG. 1. Typical SANS profiles of DPPC-d_9 in its three phases obtained on cooling. From top to bottom, data within the $L_{\beta'}$ (gel) at $T = 20\,°C$, $P_{\beta'}$ (ripple) at $T = 39\,°C$, and L_α (liquid crystal) phases at $T = 45\,°C$.

DPPC sample was prepared in the D_2O buffer following the same procedure. The DPPC sample used in the x-ray samples were prepared in a similar manner except with H_2O substituted for the D_2O. The x-ray samples were placed in 1.5 mm diameter $\varnothing$ glass capillaries and visually inspected before use to ensure that they satisfied the excess water condition.

The SANS experiments were conducted at the W. C. Koehler 30 m SANS facility at the Oak Ridge National Laboratory [7] using neutrons of wavelength 4.75 Å ($\delta\lambda/\lambda \sim 5\%$). Two configurations of the instrument were employed with sample-to-detector distances of 3.5 m ($Q \in [0.019, 0.17 \text{ Å}^{-1}]$) and 8.0 m ($Q \in [0.008, 0.075 \text{ Å}^{-1}]$), for relatively low- and high-resolution measurements, respectively. The SANS data were corrected for instrumental backgrounds and detector efficiency and converted into absolute differential cross sections per unit sample volume using established protocols [8,9].

As a complement to the neutron work, x-ray diffraction experiments were conducted using Cu $K\alpha$ radiation from an 18 kW rotating anode generator which was further monochromated using a pyrolytic graphite monochromator. The resolution of the x-ray measurements was roughly a factor of 2 better than that of the neutron measurements at a sample-to-detector distance of 3.5 m, which allowed fine structure within the diffraction pattern to be resolved. While neutrons and x rays are similar diffraction probes, neutrons scatter from the nuclei in atoms while x rays scatter off the electronic charge distribution, and consequently the use of the two techniques in tandem is expected to yield complementary information regarding the same structure.

III. RESULTS AND DISCUSSION

A. Experimental results

Figure 1 shows the low-resolution (3.5 m) SANS diffraction pattern for DPPC-d_9 in three different phases obtained on cooling. The phases are clearly distinguished by the shift in the lamellar repeat peak and the changes in the scattering intensity below $Q = 0.05 \text{ Å}^{-1}$. The evolution of the diffrac-

tion pattern as a function of temperature can be better appreciated when presented as a contour plot, as shown in Figs. 2 and 3 for the warming and cooling runs, respectively.

Figure 2 shows a color contour plot of low-resolution neutron data taken while slowly warming the DPPC-d_9 from 20 °C to 55 °C. Data collection began five minutes after the temperature had stabilized to within ± 0.1 °C of the target temperature, following a change in temperature. Each measurement set was taken over a period of 30 min. Temperature steps of 0.5 °C were taken in the range from $T = 31$ °C to 43 °C. Additional measurements were also performed before and after the main measurement at one temperature in each phase for comparative purposes in order to ensure that relaxation kinetics were not affecting the results. No such effect was observed at any temperature.

The three phases of DPPC in the temperature range shown in Fig. 2 are easily identified by the rather abrupt changes in the overall pattern, including a shift in position of the lamellar repeat peak and dramatic changes in the the very low angle scattering $[Q = (4\pi/\lambda)\sin\theta < 0.03 \text{ Å}^{-1}]$. This latter scattering increases strongly upon entering the $P_{\beta'}$ phase from the $L_{\beta'}$ phase and subsequently falls in the L_α phase. The inset shows data from a separate, higher-resolution (8.0 m) experiment conducted to examine the region enclosed by the white box in Fig. 2.

Neutron scattering profiles of DPPC-d_9 as the same sample was slowly *cooled* are shown in Fig. 3. Similar thermal protocol as described above was employed. The scattering due to the ripple periodicity in the $P_{\beta'}$ phase ($Q \sim 0.05 \text{ Å}^{-1}$) is much more prominent on cooling and the low angle scattering is markedly different. In the cooling scans, the very low-Q scattering in the $P_{\beta'}$ phase, while more intense than that of the L_α phase, does not approach the levels attained in the warming scans and reaches its highest intensity in the $L_{\beta'}$ phase. The undeuterated DPPC sample displayed similar scattering profiles which are not shown in this paper.

Figure 4 shows the complementary x-ray and neutron diffraction patterns obtained by these two techniques for DPPC warmed into the $P_{\beta'}$ phase. Both data sets were taken at $T = 39$ °C and the x-ray data have been scaled arbitrarily so that the data sets overlap. The lamellar repeat peak at $Q = 0.086 \text{ Å}^{-1}$ exhibits roughly the same width in both data sets, indicating that this is a single Bragg-like feature whose intrinsic width implies the presence of disorder. The neutron data also show a shoulder related to the ripple periodicity near $Q = 0.05 \text{ Å}^{-1}$ which does not appear in the x-ray profile corresponding to a ripple wavelength of $\lambda_r \sim 125 \text{ Å}$ in the ripple phase on warming, in agreement with previous freeze-fracture measurements [10] but slightly less than previous x-ray diffraction results [6,11]. In contrast, the data shown in Fig. 5, collected after cooling slowly into the $P_{\beta'}$ phase from the L_α phase, show an enhanced neutron peak from the ripple periodicity near $Q = 0.05 \text{ Å}^{-1}$ and the peak attributed to the lamellar repeat appears much broader. The higher-resolution x-ray cooling data show that this broad peak is, in fact, made up of two closely spaced peaks at $Q = 0.072$ and 0.087 Å^{-1} that are not fully resolved by the neutrons. In addition, the x-rays reveal a peak at $Q = 0.10 \text{ Å}^{-1}$ which does not appear in the neutron profile.
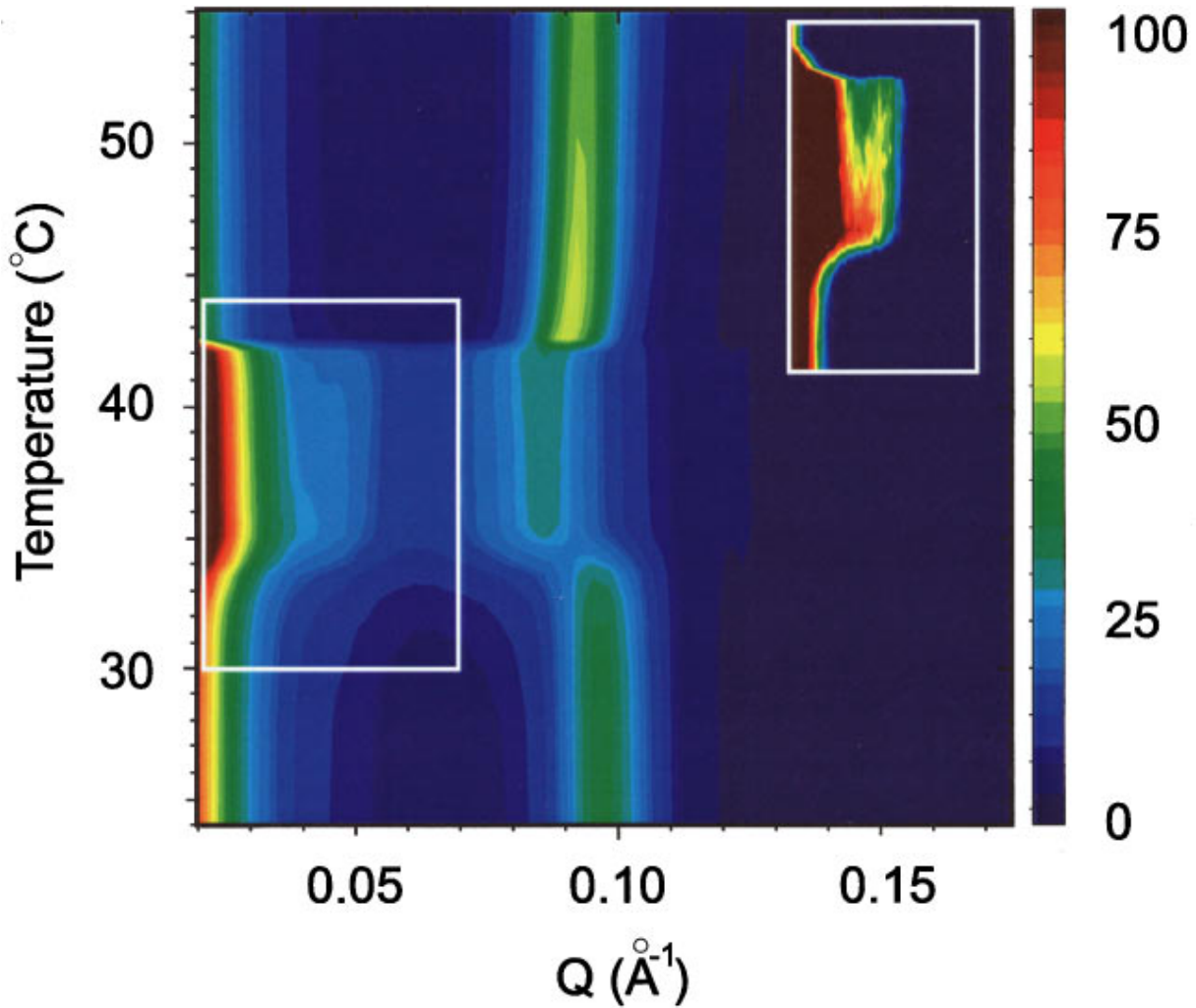
FIG. 2. (Color) Color contour plot of DPPC-d_9 in excess water warming through its three phases ($L_{\beta'}, P_{\beta'}, L_\alpha$) in this temperature range. The main plot shows neutron data taken with a sample-to-detector distance of 3.5 m ($Q \in [0.019, 0.17 \text{ Å}^{-1}]$). The inset shows data from a separate, 8.0 m experiment corresponding to the region enclosed by the white box ($Q \in [0.02, 0.075 \text{ Å}^{-1}]$).

B. Modeling the ripple phase

It is well known [1,12] that the ripple phase can be described by a two-dimensional monoclinic lattice, shown schematically in Fig. 6, where the unit vectors are given by

$$\vec{a} = d \cot \gamma \, \hat{x} + d\hat{z} \quad \text{and} \quad \vec{b} = \lambda_r \, \hat{x}, \tag{1}$$

where d is the lamellar repeat distance, λ_r is the ripple wavelength, and the difference between γ and 90° is a measure of the monoclinicity. The reciprocal lattice vectors are then

$$\vec{A} = \frac{2\pi}{d} \, \hat{z} \quad \text{and} \quad \vec{B} = \frac{2\pi}{\lambda_r} \, \hat{x} - \frac{2\pi}{\lambda_r \tan \gamma} \, \hat{z}. \tag{2}$$

The absolute form factors reported by Wack and Webb [12] for the $P_{\beta'}$ phase of the related phospholipid DMPC suggest that the strongest peaks for the low-Q range should correspond to the $(1\bar{1})$, (10), and (11) reflections. If we assume that these reflections are peaks 2, 3, and 4, respectively, in Fig. 5, we must conclude that peak 1 is the (02) reflection in order to obtain reasonable values for our unit cell. These assignments give $d = 73$ Å in agreement with the value obtained on warming and with other measurements [12], λ_r

$= 330$ Å, and $\gamma = 126°$. Long wavelength ripples of this order have been reported previously but not with an accompanying large monoclinicity [6,13].

A consequence of our assignment of peak 1 in Fig. 5 as the (02) reflection is that we should expect to see the (01) reflection at a Q value half that of (02). Figure 7 shows the high-resolution (8 m) neutron profile of DPPC-d_9 at 39 °C within the $P_{\beta'}$ phase on cooling, along with a nonlinear least squares fit to the data. The pattern could not be adequately fit with a power law background and a single Lorentzian centered at $Q \sim 0.05 \text{ Å}^{-1}$, but the addition of a second Lorentzian at half this Q value describes the data well. The inset shows the same cooling data on a semilog scale, along with the corresponding profile obtained on warming. In this plot the (01) peak is clearly discernible in the raw data of the cooling scan and is absent in the warming data.

Figure 8 shows the x-ray diffraction profile of DPPC in the $P_{\beta'}$ phase on cooling taken from Yao *et al.* [6]. As already discussed, these authors interpreted this profile as the superposition of two different rippled regions, each with its own ripple wavelength, bilayer periodicity, and monoclinicity. However, the single, long wavelength ripple phase model which we constructed to describe our diffraction data *also*
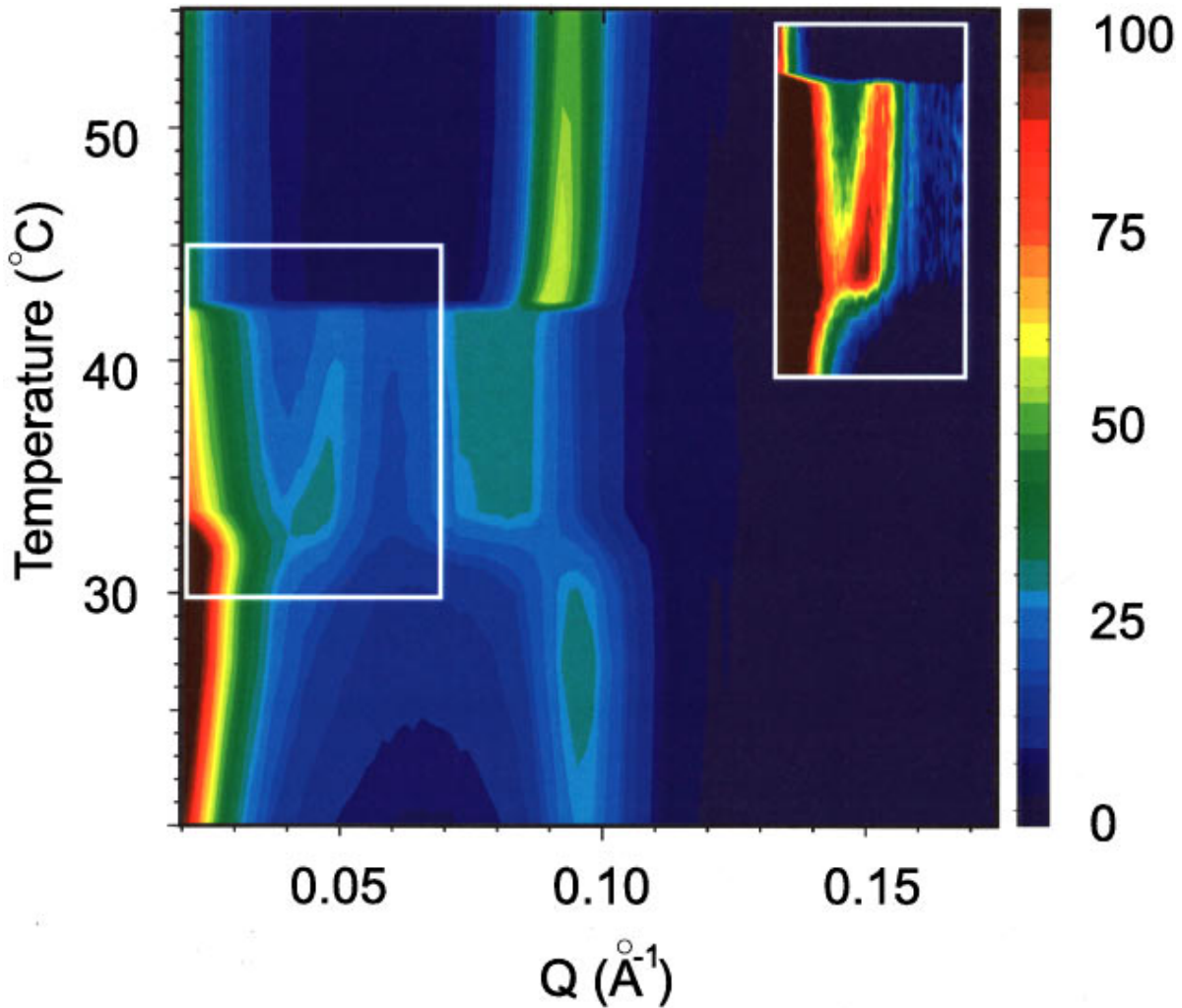
FIG. 3. (Color) Color contour plot of DPPC-d_9 as in Fig. 2, but with the sample slowly cooled through this temperature range.

describes their diffraction data. This can be seen in Fig. 8 and Table I, where we directly compare the measured and calculated peak positions using a model structure for which $\lambda_r = 350$ Å, $d = 71$ Å, and $\gamma = 129°$. These results agree well with the results from our experiments, with the greatest dis-

crepancy being a 6% difference in the ripple wavelength. The vertical lines in Fig. 8 indicate the calculated peak positions of the Bragg reflections in the given range. Only reflections up to third order are shown. The measured and calculated peak positions are summarized in Table I. This yields
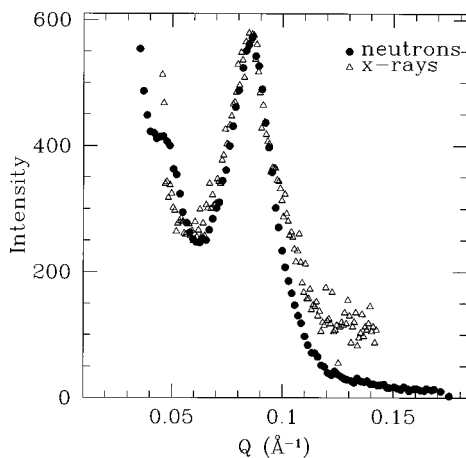

FIG. 4. A comparison of neutron and x-ray scattering profiles of DPPC-d_9 in the $P_{\beta'}$ phase (both at $T = 39$ °C) after warming from the $L_{\beta'}$ phase.

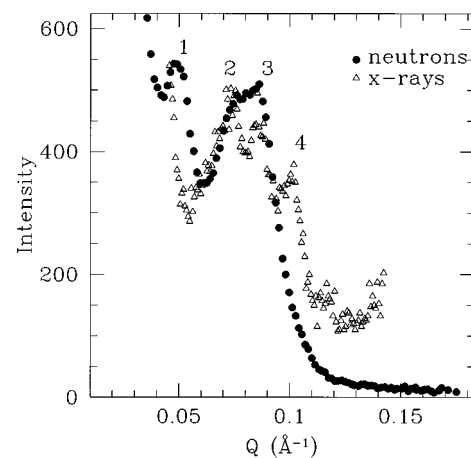
FIG. 5. A comparison of neutron and x-ray scattering profiles of DPPC-d_9 in the $P_{\beta'}$ phase (both at $T = 39$ °C) after slow cooling from the L_α phase.
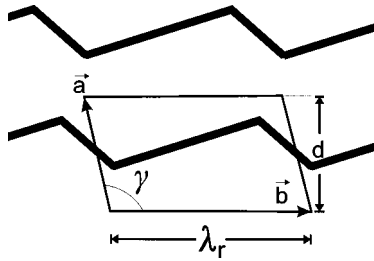
FIG. 6. A schematic drawing of the monoclinic unit cell of DPPC in the $P_{\beta'}$ phase. The cell is uniquely defined by the bilayer periodicity d, ripple wavelength λ_r, and monoclinic angle γ.

an excellent description of the Yao et al. [6] data. The single phase structure we suggest is also consistent with the decrease in diffuse scattering observed at small Q compared with the ripple phase obtained on warming. A superposition of two rippled structures would be expected to give rise to increased diffuse scattering due to disorder, which is not observed.

C. Temperature dependence of the ripple phase

Figure 9 shows a fit to the low-resolution (3.5 m) neutron data in the $P_{\beta'}$ phase, cooled from the L_α phase. Consistent with the relevant x-ray data (Fig. 5) where three peaks are resolved, the broad peak in the neutron profile consists of two distinct reflections which we have labeled $(1\bar{1})$ and (10). A fourth peak was necessary in order to match the data in the tail ($Q > 0.95$ Å^{-1}) of the broad feature. This peak likely corresponds to peak 4 in the x-ray data (Fig. 5) although it appears to be centered below its x-ray value of $Q = 0.10$ Å^{-1}. The small amplitude of this peak in the neutron data and its proximity to the strong $(1\bar{1})$ and (10) peaks makes it difficult to extract any reliable information about this peak from the neutron profile. The behavior of the remaining three peaks, however, can yield useful information as demonstrated in Fig. 10, which traces the (02) and (10)
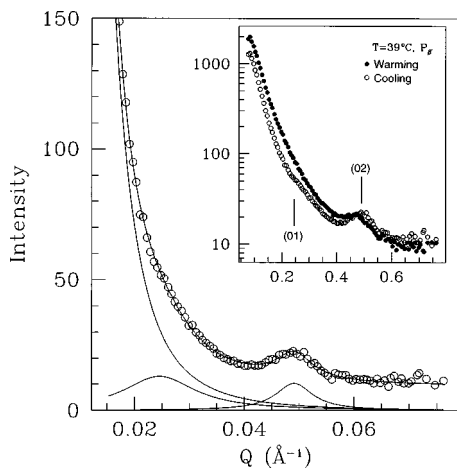

FIG. 7. A fit to the high-resolution (8.0 m) neutron data of DPPC-d_9 in the $P_{\beta'}$ phase is shown. The main plot shows the data on a linear scale along with the fit. The three components of the fit, the power law background and two Lorentzians, are also included. The inset compares the profiles of the $P_{\beta'}$ phase obtained on warming and cooling on a semilog scale.
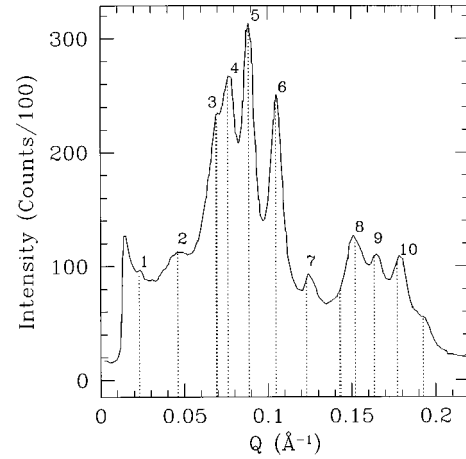

FIG. 8. X-ray diffraction profile of DPPC in the $P_{\beta'}$ phase on cooling (taken from Yao et al. [6]). The vertical lines indicate expected peak positions calculated using our model and detailed in Table I.

peak positions as a function of temperature through the ripple phase on cooling. The top two panels show the peak position and amplitude, respectively, of the (02) reflection as extracted from fits to the high-resolution (8.0 m) neutron data. The bottom panel shows the peak position of the (10) taken from fits to the low-resolution (3.5 m) data. It should be noted that the (10) data have been shifted by 1.0 °C along the temperature axis to ensure a match between the transition temperatures for the high-resolution and low-resolution experiments since it was found that the pretransition temperature for these two separate experiments differed by this amount.

Equation (2) shows that the change in position of the (02) peak as a function of temperature could be the result of either

TABLE I. Calculated and measured peak positions of DPPC in the $P_{\beta'}$ phase on cooling. Peak numbers correspond to the labels shown in Fig. 8. Only reflections up to third order are shown. The question marks in the ''Peak Number'' column correspond to calculated reflections which were not labeled in the work of Yao et al. [6].

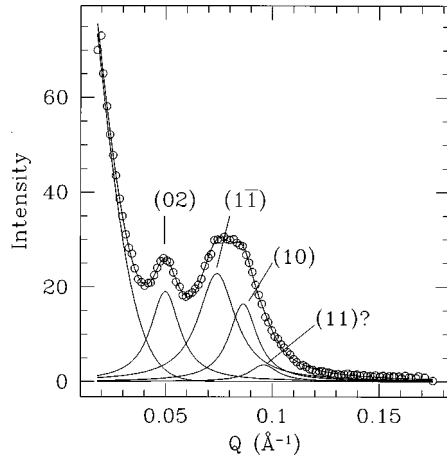| Peak number	Peak label (hk)	Calculated (Å^{-1})	Measured (Å^{-1})
1	(01)	0.023	0.023
2	(02)	0.046	0.046
3	(03)	0.069	0.070
	$(1\bar{2})$	0.069	
	$(1\bar{3})$	0.070	
4	$(1\bar{1})$	0.076	0.077
5	(10)	0.089	0.089
6	(11)	0.118	0.119
7	(12)	0.123	0.124
?	(13)	0.143	
	$(2\bar{3})$	0.144	
8	$(2\bar{2})$	0.152	0.152
9	$(2\bar{1})$	0.164	0.164
10	(20)	0.177	0.178
?	(21)	0.193	

FIG. 9. Fit to the low-resolution (3.5 m) neutron data of DPPC-d_9. The fit consists of a background power law term and four separate Lorentzians. The Lorentzian associated with the (11) peak falls within the tails of the $(1\bar{1})$ and (10) peaks, making it difficult to extract any reliable information about its position.

FIG. 11. Temperature dependence of the $(1\bar{1})$ peak in DPPC-d_9 in the $P_{\beta'}$ phase on cooling. The dashed lines indicate the expected temperature dependence of the $(1\bar{1})$ peak using two simple models and the observed temperature dependence of the (10) and (20) peaks. The results clearly show λ_r to be changing with temperature while the monoclinicity remains constant.

a temperature dependent ripple wavelength λ_r or monoclinicity γ, or both. Using the measured temperature dependence of the (02) and (10) peaks, we can predict the temperature dependence of the $(1\bar{1})$ peak under the two possible limiting assumptions (λ varies, γ constant, or γ varies, λ constant) about our unit cell. As can be seen in Fig. 11, a model in which γ is held constant and λ_r varies with temperature is a good description of the observed data, while one in which λ_r is fixed and γ is allowed to vary is not.

As the origin of the temperature dependence of the (02) peak position within the $P_{\beta'}$ phase has been identified as being due to λ_r, it is interesting to compare the thermal expansivity observed in the middle of the ripple phase on cooling with that typically observed in "hard" materials near room temperature. The thermal expansivity is defined as $\alpha = (1/a)(da/dT)$ where a is the appropriate lattice param-
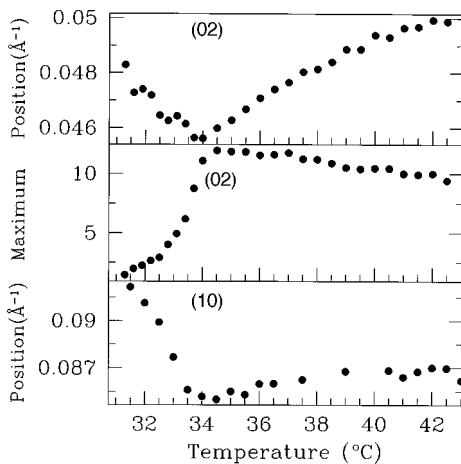
FIG. 10. Temperature dependence of the (02) and (10) peaks in DPPC-d_9 in the $P_{\beta'}$ phase on cooling. The top two panels show the (02) peak position extracted from the high-resolution neutron experiment, while the bottom panel shows the peak position of the (10) peak taken from the low-resolution neutron experiment. The temperature scale of the low-resolution (3.5 m) data has been shifted by 1 °C as the pretransition temperature differed by this amount in the two separate experiments.
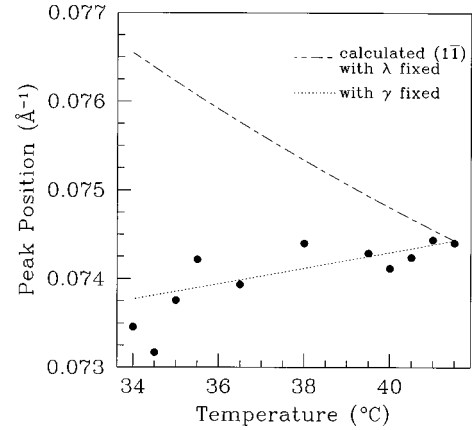
eter. For the expansivity of the ripples, we obtain a value of $\alpha \sim 0.01$ K^{-1} in the middle of the ripple phase, which is huge compared to expansivities displayed by typical "hard" materials. Near room temperature metallic cesium exhibits the largest α displayed by an element, $\alpha \sim 0.0001$ K^{-1}. This behavior is anomalously large compared with other elements, due to the fact that cesium melts just above room temperature. The ripple expansivity is sufficiently large that we feel it cannot be due to the anharmonic effects normally ascribed to thermal expansion, but rather to a temperature dependent penetration of the water into the head group region of the rippled bilayer, expanding the ripple structure out within the plane of the bilayer.

D. Stability of the ripple phase

Given that two $P_{\beta'}$ phases are clearly observed, one on warming and one on cooling, the question of which one is the equilibrium and which one is metastable remains. On the basis of calorimetric measurements of the enthalpies of the phases, Tenchov, Yao, and Hatta [5] concluded that the ripple phase on cooling is metastable but long lived, and that the $P_{\beta'}$ phase achieved on warming is the true equilibrium phase. This conclusion is premature without entropic information about the two states. There are two features in the comparison between the scattering in the two ripple phases which lead us to believe that the $P_{\beta'}$ phase obtained on cooling is the more ordered phase. First, it displays much less diffuse small-angle scattering than does the ripple phase obtained on warming from the $L_{\beta'}$ phase, as is clearly seen in the inset of Fig. 7. Second, the Bragg peaks are sharper in the $L_{\beta'}$ phase obtained on cooling. We therefore conclude that the entropy of the $P_{\beta'}$ phase on cooling is less than the entropy of the $P_{\beta'}$ phase on warming. Since our experiments are conducted at constant pressure, it is the Gibbs potential $G = H - TS$ which is relevant. Denoting the warming and cooling $P_{\beta'}$ phases with the subscripts w and c, respectively, we can now make the following simple thermodynamic argument:

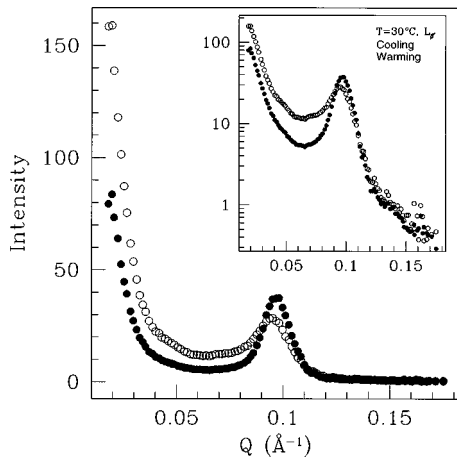$$S_c < S_w \Leftrightarrow S_w - S_c = \delta S, \quad \delta S > 0$$

FIG. 12. Comparison of the neutron scattering profiles of DPPC-d_9 in the $L_{\beta'}$ (gel) phase on warming and cooling. The inset shows the same data on a semilog scale. Both the width of the lamellar repeat peak and the intensity of the small angle ($Q < 0.09$ Å^{-1}) are enhanced in the cooling profile.

$$H_c > H_w \Leftrightarrow H_c - H_w = \delta H, \quad \delta H > 0$$

$$G_c - G_w = (H_c - H_w) + T(S_w - S_c) = \delta H + T\delta S > 0,$$

confirming the previous conclusion that the $P_{\beta'}$ phase on cooling is metastable.

We also observe, in agreement with previous measurements [14,15], that the bilayer periodicity exhibits a pronounced temperature dependence, known as anomalous swelling, just above the the $P_{\beta'}$-L_α transition temperature T_m (Figs. 2 and 3). Matuoka *et al.* [16] have shown that the appearance of the multipeak profile in the $P_{\beta'}$ phase requires slow cooling rates through the L_α phase in the vicinity of T_m. It is possible that passage through the anomalous swelling regime, with its strong temperature dependent lamellar repeat distance and concomitant reduction in bilayer curvature modulus [14] constrains the system to assume the metastable $P_{\beta'}$ structure. The system must pass through this region on cooling into the $P_{\beta'}$ phase from the fluid L_α phase, but not when the $L_{\beta'}$ phase is the temperature precursor.

E. Metastable gel phase

The color contour plot of DPPC-d_9 on cooling (Fig. 3) indicates that remnants of the ripple phase persist into the $L_{\beta'}$ phase. One can trace the path of the (02) ripple periodicity peak as it decreases in Q with the approach to the $P_{\beta'}$ to $L_{\beta'}$ transition from above. At the pretransition temperature T_p (~34 °C), the (02) ripple periodicity peak merges with the very low-Q scattering within the $L_{\beta'}$ phase, suggesting that this scattering originates from remnants of the

ripples which are frozen into the $L_{\beta'}$ phase. Explicit evidence for this is seen in Fig. 10, which shows that fits to the scattering profile include a contribution from the ripple structure below T_p and well into the $L_{\beta'}$ phase. Figure 12 depicts the essentials of this argument more clearly. Here we see the marked difference in the warming and cooling scans within the $L_{\beta'}$ phase on both linear and semilog scales. In addition to the increased scattering at all wave vectors below $Q \sim 0.09$ Å^{-1} in the cooling scan, the lamellar repeat peak is broader and less well defined than that observed in the warming profile. This indicates the presence of disorder in the bilayer periodicity which is expected as the presence of short range ordered ripple regions in the $L_{\beta'}$ phase is likely to disrupt the bilayer stacking.

IV. CONCLUSION

In conclusion, we have performed complementary neutron and x-ray scattering experiments on MLV samples of DPPC in excess water. Our measurements focused on the ripple, $P_{\beta'}$, phases and we clearly see that different ripple phases form depending on whether the phase is entered from above or below in temperature. The $P_{\beta'}$ structure is much more highly ordered on cooling than on warming, and the diffraction patterns within the ordered $P_{\beta'}$ phase obtained on cooling are well described using a simple model characterized by a single, long periodicity ripple and large monoclinicity. This model is fully consistent with previous high-resolution x-ray data of DPPC in the $P_{\beta'}$ phase on cooling.

The ripple wavelength λ_r is found to change dramatically as a function of temperature within this phase, consistent with significant alterations in the degree of penetration or local structure of the water-head group region of the bilayer, as the phase is spanned in temperature. Our data also clearly show that remnants of the ripple phase persist well past the pretransition temperature into the $L_{\beta'}$ phase, so that both the $P_{\beta'}$ and $L_{\beta'}$ ''solid'' phases display pronounced history dependencies.

[1] W.-J. Sun, S. Tristram-Nagle, R. M. Suter, and J. F. Nagle, Proc. Natl. Acad. Sci. USA **93**, 7008 (1996).

[2] H. W. Meyer, Biochim. Biophys. Acta **1302**, 138 (1996).

[3] J. Katsaras and V. A. Raghunathan, Phys. Rev. Lett. **74**, 2022 (1995).

[4] J. Katsaras, R. F. Epand, and R. M. Epand, Phys. Rev. E **55**, 3751 (1997).

[5] B. G. Tenchov, H. Yao, and I. Hatta, Biophys. J. **56**, 757 (1989).

[6] H. Yao, S. Matuoka, B. Tenchov, and I. Hatta, Biophys. J. **59**, 252 (1991).

[7] W. C. Koehler, Physica (Utrecht) **137B**, 320 (1986).

[8] G. D. Wignall and F. S. Bates, J. Appl. Crystallogr. **20**, 28 (1986).

[9] W. S. Dubner, J. M. Schultz, and G. D. Wignall, J. Appl. Crystallogr. **23**, 469 (1990).

[10] J. A. N. Zasadzinski, J. Schneir, J. Gurley, V. Ehings, and P. K. Hansma, Science **239**, 953 (1988).

[11] S. Matuoka, S. Kato, and I. Hatta, Biophys. J. **67**, 728 (1994).

[12] D. C. Wack and W. W. Webb, Phys. Rev. A **40**, 2712 (1989).

[13] H. W. Meyer, B. Dobner, and K. Semmler, Chem. Phys. Lipids **82**, 179 (1996).

[14] J. Lemmich, K. Mortensen, J. H. Ipsen, T. Honger, R. Bauer, and O. G. Mouritsen, Phys. Rev. E **53**, 5169 (1996).

[15] J. F. Nagle, H. I. Petrache, N. Gouliaev, S. Tristram-Nagle, Y. Liu, R. M. Suter, and K. Gawrisch, Phys. Rev. E **58**, 7769 (1998).

[16] S. Matuoka, H. Yao, S. Kato, and I. Hatta, Biophys. J. **64**, 1456 (1993).